

Field reconnaissance insights from the 2024 Noto earthquake

S. M. K. Pasha

Construction Solutions Development Department, GIKEN LTD., Kochi, Japan

Y. Ishihara

Construction Solutions Development Department, GIKEN LTD., Kochi, Japan

K. Toda

Construction Solutions Development Department, GIKEN LTD., Kochi, Japan

T. Nozaki

International Press-in Association, GIKEN LTD., Kochi, Japan

D. Hirose

International Press-in Association, GIKEN LTD., Kochi, Japan

M. Kato

International Press-in Association, GIKEN LTD., Kochi, Japan

T. Matsumoto

Faculty of Engineering, Kanazawa University, Kanazawa, Japan

ABSTRACT

A strong earthquake with a moment magnitude of $M_{jma}=7.6$ ($M_w=7.5$) and an epicentral depth of approximately 16 km struck the Noto Peninsula in central Japan. This seismic event caused significant damage to infrastructure, including roads, highways, residential buildings, embankments, and dikes, primarily due to earthquake-induced phenomena such as liquefaction, lateral spreading, landslides, and debris flows. Additionally, the earthquake altered the coastal landforms, with fault zone ruptures leading to up to 4 m of uplift in several regions. The authors visited the affected areas and conducted post-earthquake field reconnaissance in Kanazawa, Wajima, Nanao, Anamizu, Suzu, Noto, and Toyama, gathering crucial, time-sensitive data. The collected dataset encompasses reconnaissance track records, over 1000 geotagged photographs, ground coordinates, and various other field measurements and observations. This data, along with post-processed information on the damaged areas and structures, provides a comprehensive insight into the earthquake's impact. The information gathered by the field team, enhanced by thorough analytical efforts, provides detailed insights into the ground's morphology and movement patterns, the nature of ground failures, structural damages, and their potential causes. In contrast, many residential houses, road embankments, waterfront structures, and river embankments were partially or totally damaged due to lateral spreading and liquefaction-induced ground deformation. The findings of this reconnaissance suggest that pile-supported foundations, bridges, and waterfront sheet pile structures showed better performance and suffered minimal damage during this earthquake.

Key words: 2024 Noto earthquake, reconnaissance, Sheet pile, Liquefaction, Landslide

1. Noto Peninsula Geology

1.1. Geology framework

The Noto Peninsula's geology is a clear narrative of dynamic geologic processes, characterized by the prominence of Neozoic basement rocks, which signify its uplifted status relative to the surrounding lowlands and marine areas. Its stratigraphy is dominated by a complex interplay of Cenozoic volcanic and sedimentary units atop an older Paleozoic-Mesozoic base, including Hida gneiss and granite intrusions, which are pivotal in understanding the region's geologic evolution.

Key stratigraphic highlights include the Anamizu and Yanagida formations, which encapsulate the volcanic and sedimentary dynamics of the region. The Anamizu formation, with its diverse volcanic and sedimentary constituents, and the Yanagida formation, rich in acidic pyroclastic materials, are crucial in deciphering the volcanic history and sedimentary processes of the peninsula (Fig. 1) (AIST, 2023).

The peninsula's geologic history is marked by significant tectonic phases, with extensional deformation during the Miocene, associated with the Japan Sea's opening, and subsequent Pliocene compressional adjustments, reshaping its geologic framework. These processes, coupled with the sedimentary and volcanic interactions during the Miocene-Pliocene, offer profound insights into the peninsula's geologic past, reflecting a complex history of tectonic and sedimentary interplay that has sculpted its current geological identity. (Takeuchi, A. 2010)

1.2. Tectonics of the Noto Peninsula

The tectonic landscape of the Noto Peninsula is defined by a complex interplay of fault systems and mass movements, which have been instrumental in sculpting the region's current geological and topographical features. Among the notable faults is the Ochigata Fault, which delineates the Ochigata Plain, with its central coordinates approximately at 37.3°N latitude and 136.9°E longitude. This fault exhibits thrust faulting characteristics, with the northern segment striking at N50E and dipping at 30° to the northwest, while the southern boundary fault strikes at N40E and dips at 20° to the northeast.

In close proximity to the coastline lies the Noto Shore Fault, centered around 37.4°N latitude and 137.3°E

longitude, demonstrating a N40E strike and a 60° dip towards the northeast, indicative of its thrust nature. The peninsula's tectonic fabric is further enriched by additional active faults, including the Isurugi, Kanazawa, Takashiyozu, and Kurehayama thrust faults, each contributing to the region's dynamic geological identity.

A fault identified as F43, a reverse fault among the 60 evaluated faults, extends to the seabed just north of the Noto Peninsula, following a WSW–ENE trend. This southeast-dipping fault, comprising two segments with a total length of 94.2 km (58.5 miles), is considered capable of generating an earthquake with a magnitude of Mw 7.6. It is believed that this fault was the source of the 2024 Noto earthquake. (Fig. 2)

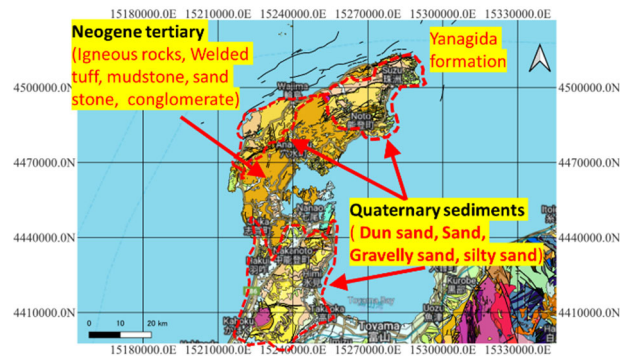


Fig. 1 Geology of Noto Peninsula (Map created using data from Geological Survey of Japan, AIST 2023)

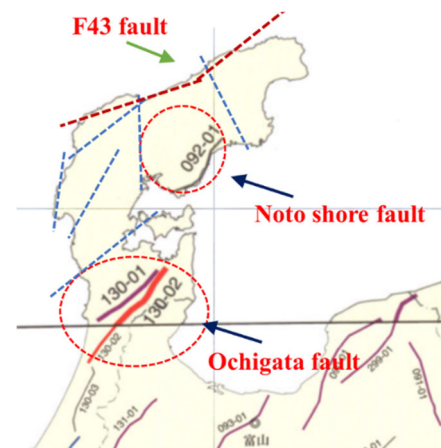


Fig. 2 Faults in Noto Peninsula (Fuji and Satake, 2024)

2. Past seismicity and recorded ground motions

2.1. Past earthquakes

Seismological records reveal that the region periodically experiences significant seismic events. Most

of these events are of the intra-plate variety. **Fig. 3** illustrates the locations of past seismic events, excluding recent ones. The region's seismicity is influenced by the convergence and interaction of multiple tectonic plates, including the Pacific, Philippine Sea, Okhotsk, and Amurian Plates. Research suggests that the predominant faulting mechanism in seismic activities around the Noto Peninsula is thrust faulting. The latest major event took place in 2007 with a magnitude measured at $M_{jma}=6.9$. The faulting mechanisms of the events in 1933 and 2007 closely resemble that of the 2024 event. As depicted in **Fig. 3**, the seismicity aligns in specific directions, typically corresponding to the known fault traces in and around the Noto Peninsula.



Fig. 3 Past major seismic events with intensity greater than 5 (Map created using data from JMA 2024)

2.2. 2024 Noto earthquake and aftershock distributions

The earthquake that struck the Noto Peninsula in 2024 occurred on the first day of January, as reported by the Japan Meteorological Agency (JMA). This seismic event took place at 16:10:22.5 local time (7:10:22.5 UTC), centered at 37°29.7'N and 137°16.2'E, with a focal depth of 16 km. Its magnitude was measured at 7.6 M_{jma} , as illustrated in **Fig. 4**. The earthquake's focal mechanism, with strikes at 47° and 215°, dips at 37° and 54°, and rakes at 100° and 82°, demonstrates a reverse fault movement along northeast-southwest oriented planes. Aftershocks identified by the Japan Meteorological Agency (JMA, 2024) spread approximately 150 km in the northeast-southwest direction. **Fig. 4** illustrates the distribution of aftershocks with a magnitude greater than 4 and their focal depths.

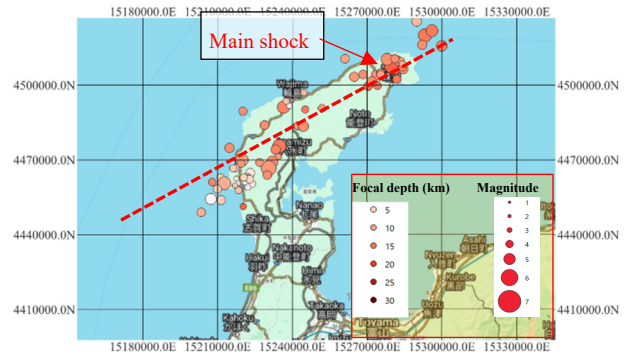


Fig. 4 2024 Noto Earthquake and Aftershocks (Map created using data from JMA 2024)

2.3. Coastal crust deformation

The 2024 Noto Peninsula Earthquake significantly altered the region's coastal landscape. SAR intensity images captured by the ALOS-2 satellite before and after the earthquake show extensive land emergence, particularly around Minazuki Bay, where the coast extended seaward by about 200m. This was due to a substantial uplift of approximately 4m in the region. Utilizing both satellite imagery and aerial photography, it was estimated that a total of 4.4 km² of new land was exposed along the coasts of the Noto Peninsula. **Fig. 5a** depicts a section of a concrete wall at Kuroshima Port in Wajima, which was raised nearly 3m. **Fig. 5b** illustrates the near-vertical and east-west directional deformation of the Earth's crust.

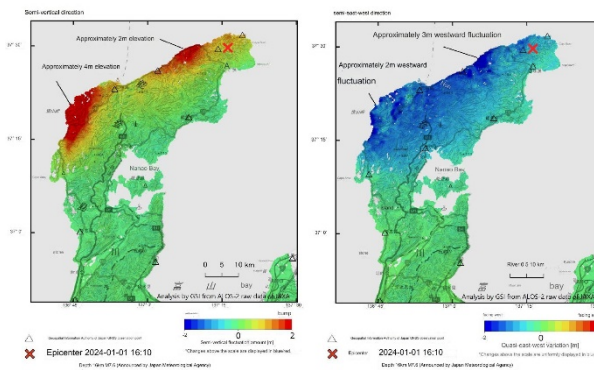
2.4. Tsunami

Following the 2024 Noto Peninsula earthquake, a major tsunami warning was issued for the Noto area, marking the first such alert since the 2011 Great East Japan Earthquake. The tsunami warnings led to immediate and urgent evacuation calls, with the first tsunami wave reaching Wajima port in less than a minute, Toyama in three minutes, and Niigata Prefecture in 21 minutes. The largest waves arrived within 11 to 26 minutes at these locations.

The tsunami generated by this earthquake had its damage concentrated mainly on the peninsula's east coast. Ground uplift in certain areas, like Wajima, acted as a natural barrier, mitigating the tsunami's impact on the northern coast.



(a)



(b)

Fig. 5 (a) Coastal crust uplift at Kuroshima Port in Wajima **(b)** Crustal deformation distribution map (Modified from GSI crustal deformation Map, 2024)

The maximum run-up heights of the tsunami were significant, reaching 3-4 meters in Suzu City and Noto Town, 1-2 meters in Toyama Prefecture, and 4-5 meters in Naoetsu City, Niigata Prefecture. In Suzu City, the tsunami inundation extended up to approximately 500 meters inland from the coast, with debris distribution providing clues to the inundation's extent and direction. Field surveys revealed the impact of the tsunami's return flow on local agriculture and infrastructure, with debris and fallen vegetation indicating the force and direction of the water. **Fig. 6** illustrates the areas impacted by the tsunami, indicated by the blue shading.

2.5. Strong ground motion

The strong motion data from the 2024 Noto earthquake were captured by the networks of the Japan

Meteorological Agency, K-Net, and Kik-Net seismographs of NIED, as well as the Port and Airport Research Institute (PARI), Building Research Institute (BRI), National Institute for Land and Infrastructure Management (NILIM), and other organizations.

Fig. 7a and **7b** illustrate the two horizontal components and the single vertical component of time histories of accelerations recorded at Togi ISK006 K-net, along with the profile and physical properties of the soil. Furthermore, **Fig. 7c** displays the distribution of peak ground accelerations (PGA) and peak ground velocities (PGV), respectively. **Table 1** lists the top ten highest horizontal PGA records, comparing them to those of the 2016 Kumamoto earthquake and the 2011 Tohoku earthquake and tsunami.

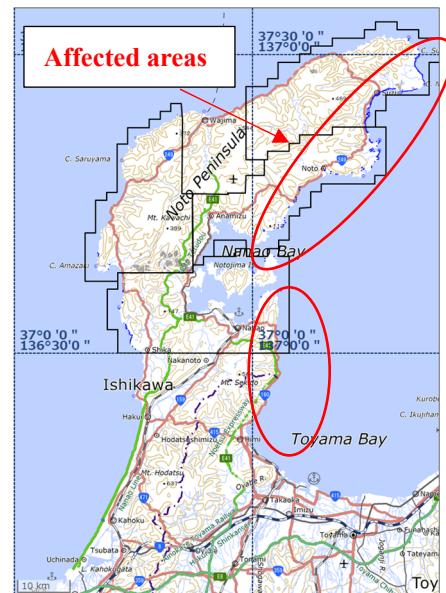


Fig. 6 Affected areas by tsunami (Data from NIED, 2024)

The maximum PGA, recorded at Togi station, was approximately 2800 gal with a duration of around 50 seconds. It is a standard practice to compare response and design spectra to assess the exceedance or non-exceedance of strong ground motions beyond the design levels. Moreover, to analyze the frequency content of the ground motion, the response spectra at four stations Togi, Wajima, Anamizu, and Suzu were compared with the Level 1 and Level 2 design response spectra for highway bridge specifications. The soil conditions are classified into three types: Type I (stiff), Type II (medium), and Type III (soft).

The damping coefficient was set at 0.05. For reference, the acceleration response spectra recorded during the 2011 Tohoku earthquake and the 2016 Kumamoto earthquake were also plotted in Fig. 8.

The acceleration response spectra at all stations exceeded the Level 1 design spectra across the entire range of natural periods. Furthermore, as observed in Fig. 8, the response acceleration exceeded the Level 2 design spectra at longer periods ($T > 1$ s) in Anamizu and Suzu, heightening the risk of damage to structures with longer natural periods, such as tall buildings, suspension bridges, and deep landslides. Conversely, at shorter periods ($T < 0.5$ s), Togi and Wajima showed exceedances, increasing the risk of damage to structures with shorter natural periods, like low-rise buildings, shear walls, and short bridges.

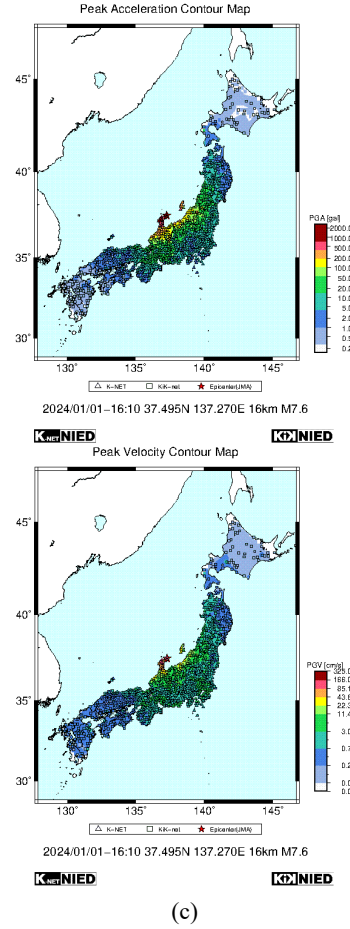
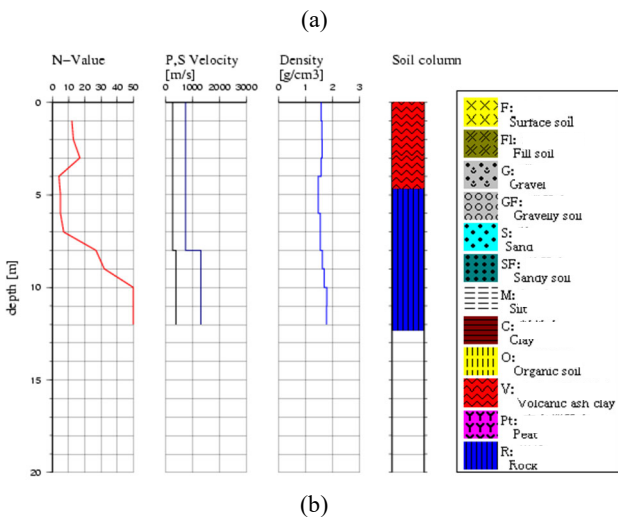
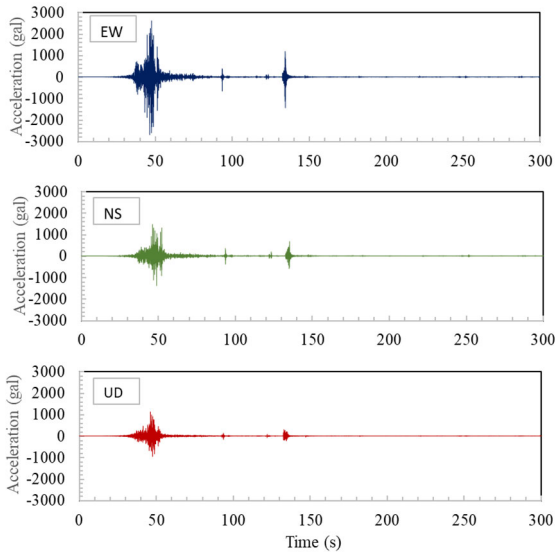


Fig. 7. (a) Time histories of acceleration at ISK006 (Togi) (b) Soil profile and physical properties at ISK006 (Togi station), (c) Peak ground acceleration and velocity distribution map (Data from NIED, 2024)

Table 1. Strong motion records obtained from National Research Institute for Earth Science and Disaster Resilience (Data from NIED, 2024)

The 2024 Noto Earthquake		The Kumamoto Earthquake (2016)		2011 Tohoku earthquake and tsunami		
No	Station	PGA (gal)	Station	PGA (gal)	Station	PGA (gal)
1	K-NET Togi (ISK006)	2828gal	KiK-net Mashiki (KMMH16)	1580gal	K-NET Tsukidate (MYG004)	2933gal
2	K-NET Wajima (ISK003)	1632gal	K-NET Yabe (KMM009)	669gal	K-NET Shiogama (MYG012)	2019gal
3	K-NET Otani (ISK001)	1469gal	K-NET Kumamoto (KMM006)	604gal	K-NET Hitachi (IBR003)	1845gal
4	K-NET Anamizu (ISK005)	1280gal	K-NET Tomochi (KMM011)	491gal	K-NET Sendai (MYG013)	1808gal
5	KiK-net Togi (ISKH04)	1220gal	KiK-net Toyono (KMMH14)	357gal	K-NET Hokota (IBR013)	1762gal
6	KiK-net Suzu (ISKH01)	1007gal	K-NET Uto (KMM008)	339gal	K-NET Imaichi (TCG009)	1444gal
7	K-NET Omachi (ISK015)	1001gal	K-NET Otsu (KMM005)	236gal	K-NET Shirakawa (FKS016)	1425gal
8	K-NET Sein (ISK002)	917gal	K-NET Takamori (KMM007)	215gal	KiK-net Saigo (FKSH10)	1335gal
9	KiK-net Shiga (ISKH06)	804gal	KiK-net Misumi (KMMH07)	173gal	K-NET Omiya (IBR004)	1312gal
10	KiK-net Yamagita (ISKH02)	791gal	KiK-net Kikuchi (KMMH03)	172gal	KiK-net Haga (TCGH16)	1305gal

3. Liquefaction and lateral spread displacements

3.1. Liquefaction induced settlements

As shown in Fig. 9a, the preliminary probabilistic distribution estimate for liquefaction due to the 2024 Noto earthquake was prepared by the National Research

Institute for Earth Science and Disaster Resilience, along with preliminary reconnaissance by the Japanese Geotechnical Society investigators.

Evidence of widespread liquefaction was found in various locations such as Wajima, Suzu, Anamizu, Nanao, Noto, and even Niigata, which is about 175 km away from the earthquake's epicenter. This was particularly noted in regions where Quaternary sediments are deposited and groundwater level is higher, such as riversides and coastal areas. Observations included sand boils, the floating of manholes, the tilting of power poles, and differential settlements.

Fig. 9b illustrates examples of free-field liquefaction sites (such as farmlands) where volumetric soil settlement and sand boils were observed. Liquefaction of reclaimed lands behind waterfront structures in ports was also observed in all previously mentioned regions.

4. Damages to structures and infrastructures

4.1. Damage to wooden buildings

Field observations indicated that wooden houses in Suzu, Wajima, and Noto experienced partial damage or complete collapse during the Noto earthquake (**Fig. 10**).

The primary failure mechanism was the hinging of wooden columns at the base and at the connections between the first and second floors, triggered by significant horizontal displacement and inertial forces. Since seismic forces acting on structures are proportional to their mass, the heavy weight of the roofs and the uneven distribution of dead loads appear to have exacerbated the extent of the damage.

Moreover, the absence of shearing walls or braces, which features like Implant™ structures in the form of sheet piles (Kondo et al., 2023) could provide, is another contributing factor to the potential damage.

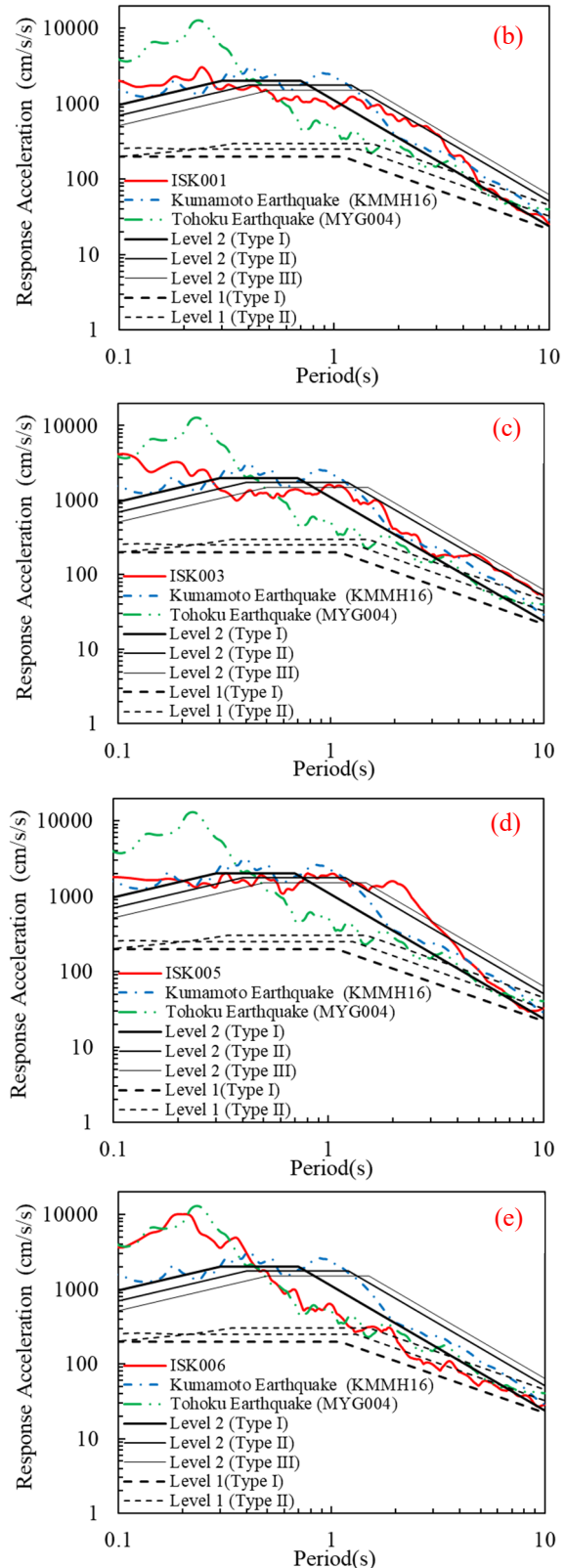
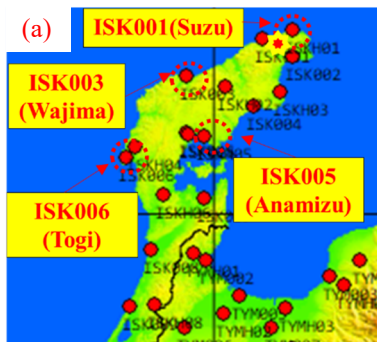
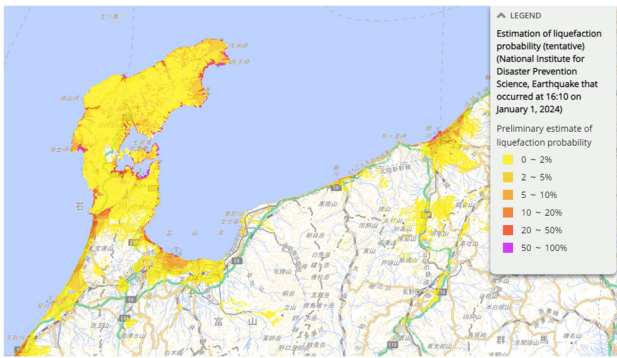


Fig. 8 (a) K-NET observation points; Acceleration response spectra of records at **(b)** ISK001(Suzu) **(c)** ISK003(Wajima) **(d)** ISK005(Anamizu) **(e)** ISK006(Togi) (Produced using acceleration records by NIED)



(a)



(b)

Fig. 9. (a) Liquefaction Susceptibility map (NIED, 2024) (b) Liquefaction induced subsidence

4.2. Damage to reinforced concrete building (RC)

Field observations indicate that reinforced concrete (RC) buildings generally exhibited good stability, with the majority sustaining minimal or no damage due to the presence of shear RC walls and pile foundations. However, there were instances where RC buildings sustained damage due to differential settlement and rotation following the onset of liquefaction or a significant loss of soil shear strength, which undermined the foundation's bearing capacity (see Fig. 11a).

An illustrative case is a seven-story RC building constructed in 1972 (see Fig. 11b) with centrifugal RC piles designed (JGS Report on 2024 Noto Earthquake) according to the 1968 Japanese Industrial Standards (JIS). This building experienced extreme subsidence on one side and uplift on the other, causing it to tip over.

Fig. 11b shows that the pile caps were separated from the pile bodies due to insufficient uplift resistance (axial capacity). The piles had an outer diameter of 35 cm and an inner diameter of 20 cm. To fully understand the overturning mechanism, an in-depth underground

investigation through excavation is necessary. For now, it can be inferred that the axial uplift capacity was likely exceeded. Considering that concrete's tensile strength is approximately 10% of its compressive strength, and once the concrete cover cracks, the pile can no longer bear any load. Therefore, steel piles might be a more viable option if the pile head connection is properly executed.

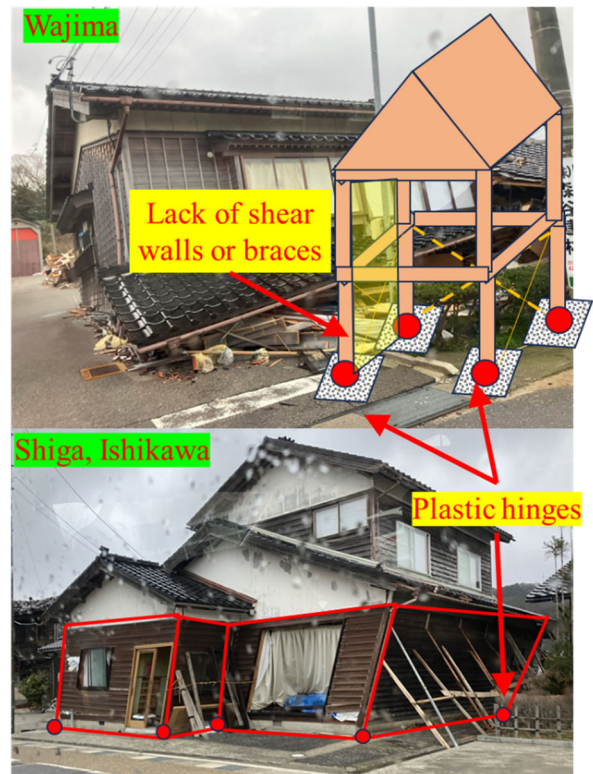


Fig. 10 Examples of Wooden structures destruction

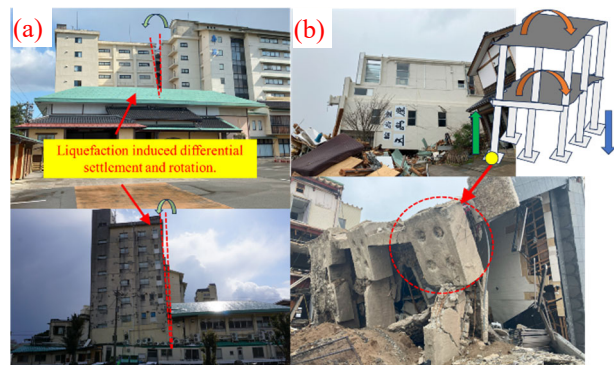


Fig. 11 (a) Liquefaction induced differential settlements and rotation (Wajima) (b) RC building collapse (Wajima)

4.3. Bridges and road embankments

Widespread landslides and debris flow were triggered by the 2024 Noto earthquake in steep volcanic

terrain. An extensive number of landslides occurred, as revealed by aerial imagery captured by the Geospatial Information Authority of Japan (GSI). **Fig. 12(a)** and **(b)** show the landslide estimates provided by the United States Geological Survey (USGS), illustrating the distribution and extent of slope failures and sediment depositions from GSI data, courtesy of the Ministry of Land, Infrastructure, Transport, and Tourism (MLIT). The correlation between the observed and estimated landslide distributions post-earthquake is notably strong. **Fig. 12(c)** displays the roads that have sustained significant damage and are either under restoration or have been restored.

Extensive landslides and ground failures, including shallow surficial slope failures over potentially weathered bedrock, complex land sliding, toppling mechanisms, and rockfalls, occurred in Nanao, Suzu, and Wajima, significantly impacting many roads and bridges in the area. These events led to the total or partial closure of roads for a while. The observations suggest that the embankment materials consisted of sandy, gravelly, and crushed rocks, which were constructed by trenching the steep slopes and using these as fill materials. As a result, they were likely loosely deposited and prone to shallow slides due to liquefaction and loss of soil shear strength. Furthermore, some roads were constructed on alluvial soil deposits, which may have led to damage caused by a reduction in the strength of the ground on which the roads were founded, either due to liquefaction or excessive vertical and horizontal deformations.

Fig. 13a illustrates an example of road embankment failure in Oyabe and Nanao. This failure was probably caused by insufficient compaction of the embankment and deep slope failure, with a horizontal distance from the head of the scarp to the canyon of approximately 200 meters over potentially weathered rock respectively.

Another example of embankment failure occurred at a twin bridge in Nanao, where the embankments on both sides of the bridge sustained damage. This was due to earthquake-induced lateral deformations, a result of the absence of a transition concrete slab between the bridge deck and the embankments, as well as a lack of adequate lateral protection, such as reinforced concrete walls or sheet piles (**Fig. 13b**).

The widespread occurrence of landslides, along with the extensive damage to roads and river embankments,

was substantial. This is also likely attributed to the large ground acceleration and site effects commonly observed in mountainous and hilltop regions.

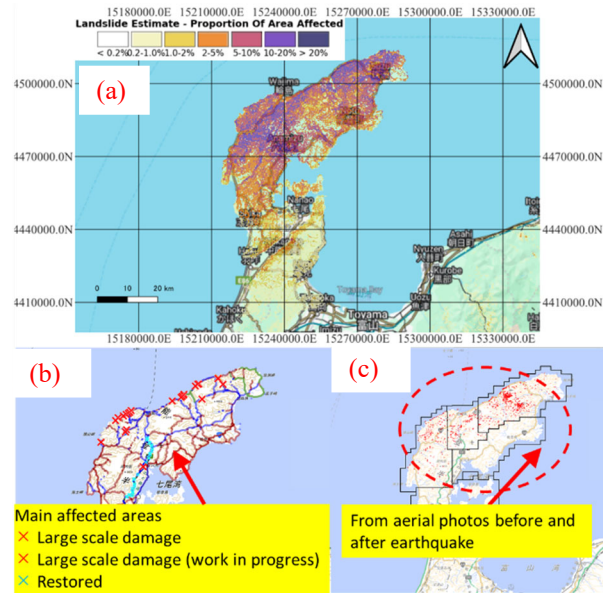


Fig. 12. (a) landslide estimates due to the 2024 Noto earthquake by the USGS (b) distribution and extent of slope failures (c) distribution of roads with significant damage



Fig. 13. (a) Road embankment failure (b) bridge embankment failure

4.4. Gravity walls, sheet piles and concrete walls

One of the primary goals of this reconnaissance was the general assessment of waterfront structures and riverside walls and sheet piles (**Fig. 14**). Some structures investigated were designed and built before the adoption of performance-based seismic design standards for ports and harbors. Before 2007, Japan's design codes for port and harbor structures relied on a prescriptive approach, specifying a single ground motion level for earthquake resistance. Notably, the criteria for Level 2 earthquakes were adjusted from a 950-year earthquake specification to a 475-year earthquake ground motion, as derived from Probabilistic Seismic Hazard Analysis (PSHA). This shift to performance-based design enhanced both the flexibility and safety of structures.

The majority of the observed waterfront structures were gravity walls (including concrete caissons and segmental block walls), concrete walls, and anchored and unanchored sheet pile walls. It was discovered that the seismic performance of these structures correlated with geotechnical conditions. There was a notable correlation between the performance of port and waterfront structures, land reclamation practices, and the apparent quality of execution. In general, reclaimed lands, especially those with substandard execution (poor compaction or ground improvement), were vulnerable to damage from liquefaction.



Fig. 14 Collapse of unreinforced concrete facing blocks and well performed sheet pile walls

In contrast, in the absence of liquefaction in the backfill or foundations, gravity walls, particularly sheet pile walls, exhibited good performance. Significant permanent deformations of gravity walls and sheet pile walls were observed in areas with widespread liquefaction.

Ground settlement in the apron area and the floating of supporting piles or gravity concrete blocks with tie rods, along with post-earthquake consolidation of loose sand, were further exacerbated by vertical displacements due to ground failures.

Sheet piles or sheet pipe piles exhibit better performance (**Fig. 14**) compared to gravity walls during earthquakes due to their enhanced flexibility and deeper penetration into the ground, which provide greater resistance to seismic forces and soil displacements, ensuring more effective stabilization and reduced risk of failure under seismic loading.

5. Conclusions

Considering the extent of damages in the affected area and the necessity for planning and executing rapid restoration plans, particularly for roads and highways, slope stabilization efforts are crucial. The application of the press-in piling method not only guarantees swift execution but also proves essential in areas with limited space available for piling procedures. For instance, during observations after the Noto earthquake, several cases of slope failure were noted, where there were residential houses situated either upstream or downstream of an unstable slope requiring immediate protection with sheet piles in constrained spaces. The zero-clearance piling method, utilizing the ZERO PILER™, offers speed and is environmentally friendly, producing neither vibration nor noise, which is crucial for the well-being of residents in the affected area.

Moreover, GIKEN Implant™, Skip Lock Method™, and Implant™ Lock Levee technologies employing SILENT PILERS™ and GYRO PILERS™ can play significant roles not only in restoration projects such as those involving road and highway embankments, waterfront structures, access bridges, dikes, and slopes, but also in countermeasure efforts. For example, using Implant™ structures to construct seismic and liquefaction-resistant residential buildings appears to be necessary. Furthermore, the investigations carried out by authors and yielded several pertinent observations regarding geotechnical phenomena and structural damage associated with the 2024 Noto earthquake as follows:

1) The region's geology significantly influenced the

frequency content of the earthquake motion at the ground surface, which in turn impacted the severity and extent of geotechnical phenomena across the Noto Peninsula.

2) The extent of landslides, as well as road and river embankment destruction, was considerable. This likely resulted from significant ground acceleration and phenomena such as site effects in mountainous and hilltop areas.

3) Liquefaction across the region led to lateral spreading, which caused damage to various structures and port facilities due to relative movements, uplift, and settlement.

4) Permanent ground deformations, coupled with ground shaking, inflicted structural damage on residential houses, buildings, bridges, and various transportation routes and utilities, including roads, highways, railways, and tollways.

5) Extreme load cases can result in the failure of structures that are otherwise considered soundly constructed. For example, landslides can trigger the catastrophic collapse of bridges or compromise well-designed residential developments. Hence, there is a critical need for slope stabilization using steel sheet piles or steel pipe sheet piles.

6) Structures such as towers, residential houses, and cranes on pile foundations have shown exceptional performance in mitigating earthquake and liquefaction-induced damages, including differential settlements and structural instability.

7) Steel sheet piles and steel pipe piles have demonstrated relatively high performance, sustaining minimal to partial damage, in protecting offshore structures against liquefaction effects.

References

- Fujii, Y., & Satake, K. (2024). Slip distribution of the 2024 Noto Peninsula earthquake (MJMA 7.6) estimated from tsunami waveforms and GNSS data. *Earth Planets Space*, 76, 44.
- Geological Survey of Japan, AIST. 2023. Seamless digital geological map of Japan V2 1:200,000. <https://gbank.gsj.jp/seamless/index.html> (in Japanese). Retrieved May 14, 2024.
- Geotechnical Society of Japan (2024). Reiwa 6 (2024) Noto Peninsula Earthquake Damage Survey Reports. Accessed April 2024. Available at: https://www.jiban.or.jp/?page_id=21412
- Goto, H. & Morikawa, H. (2012). Ground motion characteristics during the 2011 off the Pacific coast of Tohoku earthquake. *Soils and Foundations*, 52(5), pp.769-779.
- Hamada, M., Aydan, O., & Sakamoto, A. (2007). A quick report on Noto Peninsula earthquake on March 25, 2007. Japan Society of Civil Engineers Report, Tokyo.
- Ito, K., Wada, H., Watanabe, K., Horikawa, H., Tsukuda, T. & Sakai, K. (1994). 1993 Off Noto Peninsula Earthquake, Annuals, Disas. Prev. Res. Inst., Kyoto Univ., No.37, B-1, 325-341.
- Japanese Meteorological Agency (JMA) (2024). 2024 Noto Earthquake Database. Retrieved May 14, 2024.
- Katagawa, H., Hamada, M., Yoshida, S., Kadosawa, H., Mitsuhashi, A., Kono, Y. & Kinugasa, Y. (2005). Geological development of the west sea area of the Noto Peninsula district in the Neogene Tertiary to Quaternary, central Japan. *Journal of Geography (Chigaku Zasshi)*, 114(5), pp.791-810.
- Kondo, Y., Sato, K., Nishimori, Y. & Nakagawa, D. 2023. GIKEN Research Building: challenge for structure using sheet piles (part 2). *Steel Technology*, pp. 34-43 (in Japanese).
- Masuda, H., Sugawara, D., Cheng, A. C., Suppasri, A., Shigihara, Y., Kure, S. & Imamura, F. (2024). Modeling the 2024 Noto Peninsula earthquake tsunami: implications for tsunami sources in the eastern margin of the Japan Sea. National Research Institute for Earth Science and Disaster Resilience (2024). Strong-motion seismograph networks (K-NET, KiK-net).
- National Research Institute for Earth Science and Disaster Resilience (2024). Disaster Prevention Crossview of Reiwa 6 (2024) Noto Peninsula Earthquake.
- Quick report of preliminary reconnaissance of the 2024 Noto-hanto Earthquake in Japan, Japan Geotechnical Society (JGS) report, Jan 2024(in Japanese).
- Takeuchi, A. 2010. Geologic structure and late Cenozoic evolution of the Hokuriku and Shin'etsu regions, north-central Japan. *Journal of the Geological Society of Japan*, 116(11), 624-635.